Puumala Hantavirus: an imaging review.

MD Olivier Lebecque (first author, corresponding author)

Affiliation : Université catholique de Louvain, CHU UCL Namur, Department of Radiology

1 Avenue Dr G Thérasse, 5530, Yvoir, Belgium

olivier.lebecque@uclouvain.be

MD Michaël Dupont (last author)

Affiliation : Université catholique de Louvain, CHU UCL Namur, Department of Radiology

1 Avenue Dr G Thérasse, 5530, Yvoir, Belgium

michael.dupont@uclouvain.be

Abstract

Puumala virus (PUUV) is the most common hantavirus in Europe. It is known to cause nephropathia epidemica which is considered a mild type of haemorrhagic fever with renal syndrome (HFRS). However, it does not only involve kidneys, and is rarely accompanied by symptomatic haemorrhage. We review the imaging abnormalities caused by PUUV infection, from head to pelvis, emphasizing the broad spectrum of possible findings and bringing further support to a previously suggested denomination “Hantavirus disease” that would encompass all clinical manifestations. Although non-specific, knowledge of radiological appearances is useful to support clinically suspected PUUV infection, before confirmation by serology.

Keywords

Hantavirus; hemorrhagic fever with renal syndrome; Puumala virus; review

Introduction

Hantaviruses are enveloped RNA virus each carried by a specific rodent species (1). The most common Hantavirus in Europe is Puumala virus (PUUV), belonging to the Hantavirus genus of the Bunyaviridae family (2). The virus has been named after the region of Puumala, Finland, where were collected bank voles–its rodent host–which permitted to detect specific antigen for the first time in 1980 (3). Humans are usually infected from aerosolized rodent excreta when working with hay and crops during harvesting, cutting wood inside dusty wood sheds, cleaning cellars, barns or summer cottages (4). PUUV causes nephropathia epidemica (NE) which is a mild form of haemorrhagic fever with renal syndrome (HFRS) (5). The incubation period is 2-4 weeks. Typically, the course of NE has been divided into febrile, hypotensive, oliguric, diuretic, and convalescent phases, but these phases are not always clinically evident. NE presents most commonly with fever, headache, gastrointestinal symptoms (including abdominal pain), impaired renal function, and blurred vision (1). Typical laboratory findings include an increase in serum creatinine concentration, proteinuria, hypoproteinaemia, thrombocytopenia and elevation of serum C-reactive protein level (1,5). The diagnosis of acute PUUV infection is based on the detection of virus-specific IgM (1). Specific IgM antibodies can be detected in 95% of PUUV patients from their earliest serum sample, and at the latest on the 6th day after onset of illness (4,6,7). From the seroprevalence and incidence, it has been calculated that only 20-30% (8) or even less than 10% (9,10) of infected humans experience clinical problems severe enough to seek medical attention leading to serological confirmation. Over the past decades, hantavirus outbreaks have been increasing. It might be explained by better clinical awareness, development of sensitive diagnostic tests, research on reservoir, or changing climatic conditions (4,11,12).

When patients infected by PUUV are admitted to the hospital, the differential diagnosis is broad (13). A study mentioned that the initial diagnosis made by the referring physicians was

correct in less than one-third of the NE cases. As the most common symptoms of the patients are rather nonspecific, it is quite understandable (5). And this might lead the physicians to perform various diagnostic procedures, including imaging studies (13). We reviewed literature focusing on imaging findings specifically caused by PUUV infection.

Neuroradiological findings

Pituitary gland

In an acute setting, pituitary gland involvement in NE patient include pituitary oedema (14,15) and pituitary haemorrhage. A study reported that the pituitary height on brain MRI was consistent with oedema when larger than 6 mm in sagittal plane during infection (mean 7.2 mm) in 20 of 45 patients —two of whom also had pituitary haemorrhage—, and was a mean of 4.9 mm in a control MRI (mean reduction of 2.3 mm, $p<0.001$) (14). Few cases of NE complicated by pituitary haemorrhage demonstrated by brain MRI or at autopsy have been reported. Some of these patients suffered transient and complete loss of vision with severe headache (16–19), which should alert the clinician to consider the possibility of pituitary injury in a NE patient (16). When performed, brain MRI showed an increased signal intensity and enlargement in T1-weighted sagittal and coronal images, consistent with haemorrhage in the pituitary gland (Figure 1) (14,16,19). Patients with pituitary haemorrhage developed transient or permanent panhypopituitarism. These patients being more often young males, a brain MRI and hormonal studies have been recommended at least in young male patients with severe NE (18). The mechanisms of pituitary haemorrhage remain unclear. Increased permeability during acute infection, direct infection by the hantavirus or presence of the PUUV in the cerebrospinal fluid have been suggested to explain these findings (14,16,17). In other cases, disseminated intravascular coagulation, hypovolemic shock, or auto-immune mechanism have been suggested to explain pituitary injury (19–21).

As a late complication of previous NE, patients can present with hypopituitarism. Brain MRI or CT can show empty sella with pituitary atrophy (22,23) or an atrophic adenohypophysis with a heterogeneous, low signal intensity, compatible with a sequela of hypophysitis (20). However, some studies reported no abnormal imaging findings in patients with hormonal defects following NE (21,24). They suggest that the secondary hormone deficiencies found in their NE patients developed by mechanisms other than an acute haemorrhagic disruption of the pituitary (24).

Cytotoxic Lesion of the Corpus Callosum (CLOCC)

There are few case reports of patient with CLOCC associated with acute PUUV infection (25–27). Previously called “mild encephalopathy with reversible splenial lesions”, “reversible splenial lesion syndrome” or “reversible splenial lesions”, Starkey et al. recently termed these splenial lesions CLOCC. They are secondary lesions that have been associated with various conditions, including drug therapy, malignancy, infections, subarachnoid haemorrhage, metabolic abnormalities, and trauma (28). When magnetic resonance imaging is performed, axial diffusion-weighted images show a high signal intensity in the splenium of corpus callosum at high b-value with low apparent diffusion coefficient values (Figure 2). Axial T2-weighted and FLAIR images show a slight hyperintense signal at the same location. Being familiar with the imaging appearance of CLOCC might help to avoid a misdiagnosis of ischemia (28).

Acute Disseminated Encephalomyelitis (ADEM)

We found 2 reports of acute disseminated encephalomyelitis in association with NE. A brain CT revealed wide areas of hypodensity only in the periventricular white matter in one case,

and bilateral wide areas of hypodensity in the white matter partially involving the cortex in the other case. The T2-weighted brain MRI showed bilateral areas of increased signal intensity located in centrum semiovale, limited to the white matter in one case and bilateral areas of increased signal intensity located in the parietooccipital region extending to the frontal, temporal, and pons regions, also involving the cortex in the occipital region, with cerebral oedema in the other case (29,30).

Myopic shift

Ultrasonographic measurements have demonstrated anterior chamber depth of the eyes was shallower and the lens thicker in the acute phase of NE than after recovery in patients with myopic shift of 0.5 D or more (31). Ophthalmological examinations show similar findings (15,18). However, these sub millimetric changes seem to have limited implications in clinical practice.

Chest imaging findings

Pulmonary involvement

Chest x-ray has previously been reported to show abnormalities in 10-67% of NE patients (5,32–38). Abnormal chest radiograph is therefore considered common (39). The most frequent findings are pleural effusion (9.5-50%) and atelectasis (11-58%) (5,35–37,40), followed by opacities (5,34–36), cardiac enlargement (5,35,36), venous stasis (36), and pulmonary oedema (5,36) (Figure 3). Those findings have been reported to be non-disease-specific (37). Respiratory involvement has commonly been attributed at least in part to fluid overload as a result of renal failure (41,42). Patients with radiological abnormalities have been reported to be older (37 vs 40 years) than those without (34).

Only few papers studied abnormal CT/HRCT findings (37–39). The most frequent findings are pleural effusion, atelectasis and opacities. In addition, it showed intralobular reticulations and interlobular septal thickening, followed by GGO (Figure 4). Like chest radiograph abnormalities, those findings have been considered not to be disease-specific (37). One prospective study reported pulmonary oedema in 21% of their patients, and almost no opacity (4%), no GGO, neither atelectasis (39).

In America, hantaviruses–strains other than PUUV–are known to cause hantavirus pulmonary syndrome (HPS) which is characterised by acute respiratory distress, non-cardiogenic pulmonary oedema and severe hypotension (36,43). While PUUV infection is associated with mortality rates <1% (4,8), HPS is associated with a mortality rate of 38% (44). Case reports of adult respiratory distress syndrome (ARDS) mimicking HPS in PUUV infected patients have been published (41,45–48). In some cases, mild or no renal impairment was present at the time of admission, whereas the respiratory involvement was early and severe, consistent with ARDS (41,46). When performed, chest CT-scans show pronounced abnormalities including diffuse bilateral interstitial and/or alveolar opacities, dependant atelectasis with or without moderate pleural effusions (41), noncardiogenic interstitial pulmonary oedema (47), or bilateral GGO (46,47).

Cardiac imaging

In a prospective study, electrocardiogram (ECG) changes were observed in 57% of patients and considered common during acute viral infection without necessarily indicating clinical myocarditis. Echocardiography was abnormal in 16% of patients. It showed left ventricular contraction abnormalities more frequently than mild pericardial effusion. Abnormal echocardiography findings could suggest myocarditis but there was no sign of cardiomyocyte

damage (35). In another study, the main echocardiographic findings in patients during the acute phase were significantly higher pulmonary vascular resistance, higher systolic pulmonary artery pressure, lower left ventricular ejection fraction, impaired left atrial myocardial motion and a significantly higher heart rate (39). No patient was formally diagnosed with myocarditis, in these 2 studies (35,39). However, cases of myocarditis associated with PUUV have been previously reported (5), including fatal cases with myocarditis confirmed by autopsy (17). A recent case report confirmed myocarditis in a PUUV-infected patient with multiparametric cardiac magnetic resonance (CMR) combining late gadolinium enhancement with T1- and T2-mapping techniques. Considering ECG and echocardiography provide often inconclusive results, they suggest this type of CMR protocol is an adequate tool for detection and follow up of patients with hantavirus-induced myocarditis (49).

Abdominal imaging findings

Kidneys

As its name suggests, nephropathia epidemica is commonly associated with kidney involvement. Indeed, acute renal failure has been reported in up to 90% of hospital-treated patients (1,5,32,50). The typical renal histopathological lesion in NE is acute tubulointerstitial nephritis (50). Ultrasonography (US) of kidneys and bladder is the most helpful diagnostic test in patients presenting with acute kidney injury. It will assess renal size and echogenicity, exclude obstruction and doppler may be used to assess renal perfusion (51). Not surprisingly, most studies report US findings. In the largest retrospective study, renal US changes were reported in 47% of the patients. Increased cortical echogenicity (37%) and increased cortical parenchymal thickness (28%) were the most common findings, followed by patchy pattern in cortical echotexture (16%), decreased corticomedullary border differentiation (15%), and

perirenal or ascites fluid (2%) (36) (Figures 5 and 6). In a prospective study with 23 hospital-treated NE patients, quantitative renal US changes were reported in every patient between a first US examination performed on admission to the hospital and a second at a mean 140 days from onset. The length was greater in the first as compared to the second study in all patients (5-23 mm). The mean renal cortical parenchymal thickness was greater in the first as compared to the second study in 19 patients (1-12 mm). The mean renal RI was higher in the first investigation as compared to the second study in 18 patients and lower in 5 patients. Right and left kidneys did not differ significantly from each other. Some of the decrease in renal length during follow-up might in part suggest irreparable NE-induced parenchymal damage rather than just a return to the normal condition (52). A second paper studying qualitative US features with the same 23 patients reported abnormal findings in 87% (53), but they suggested some changes were so small that they could not always be detected in a clinical situation (40,53). Considering kidneys length, it is not surprising since the normal range is large, correlated with height and body mass index (54,55). Renal volume has also been reported to be significantly larger in men than in women (55). It may explain limitations associated with kidneys size assessment in a clinical situation. Finally, renal US findings are not disease specific in NE (40).

A prospective study reported renal MRI findings in NE patients. Two MRI examinations were performed in 20 consecutive patients, the primary on admission and the second at mean 196 days post onset of NE. Mean parenchymal volume, renal length and parenchymal thickness decreased significantly between the acute phase and a delayed MRI, with respectively a mean difference of 94 cm^3, 9 mm and 5.1 mm. Edema/fluid collections were found bilaterally in perirenal areas, inside and outside Gerota fascia in 16 patients in the primary study, with corresponding coronal FSE T2 FS increased signal intensity. Loss of corticomedullary signal differences on T1-weighted images was also reported. No disease-specific MRI finding was

found. MRI was reported to be superior to US in showing mild edema and evaluating renal parenchymal volume. Nevertheless, they conclude that US is more appropriate than MRI in NE patients because of the low cost and availability (56).

We didn't find any study reporting the abdominal CT findings in PUUV infected patients. However, in our experience, some patients presenting with acute abdominal pain of unknown origin and kidney failure have had an unenhanced CT of the abdomen (Figure 7). And it may be appropriate according to American College of Radiology (57).

Gallbladder

A Korean study reported up to 43% of patients having gallbladder-wall thickening (GBWT) of 4 mm or greater, even and diffuse, in patients with Hantaan hantavirus (non-European strain). They suggested that GBWT might be useful for determining the severity of HFRS (58). We found only two case reports of acalculous cholecystitis associated with Puumala hantavirus infections in English (59,60) (Figure 8). Both patients presented with positive Murphy's sign. However, these acalculous cholecystitis occurring in the context of viral infection usually resolve spontaneously and should not lead to unnecessary surgery. And gallbladder-wall thickening might just be another expression of plasma leakage with transient oedematous interstitial infiltration (60).

Spleen

Enlarged spleen evaluated by MRI, was shown to be a common finding during acute PUUV infection (Figure 7b). Koskela et al. reported a spleen length increased (median 129 mm) in the acute phase in 20 consecutive patients compared with a control phase (median 111 mm), 196 days later in average. The median change was a 15 mm in the spleen length (61).

However, clinical implication seems limited because, even if most healthy adult spleens are less than 12 cm long, variations exist due to height, weight and sex (62,63).

Other findings

Abdominal pain is common during HFRS, interesting 40% to 65% of adult patients (5,32,64,65). Increase in lipase levels has been reported in 15% of patients in a study looking for evidence of acute pancreatitis in NE patients. They didn't find signs of acute pancreatitis using imaging techniques and conclude acute pancreatitis should be considered if enzyme levels are more than threefold normal in association with clinical manifestation (64). Acute pancreatitis has been reported with swollen pancreas showed by ultrasonography and increased serum amylase level in another paper (21). Imaging of acute pancreatitis caused by other hantaviruses strains has been reported more commonly (66,67).

In addition to perirenal fluid accumulation, a case report mentioned periportal oedema seen on abdominal CT scan (47). CT of the abdomen demonstrating a thickened wall of the ascending colon, an enlarged caecum and enhancement of the peritoneum has also been reported, mimicking acute abdomen (30).

Conclusion

There might be confusion associated with the diversity of names for so called HFRS or NE and the different hantaviruses strains. PUUV infection is rarely accompanied by symptomatic haemorrhage and while it commonly affects kidneys, it can be associated with a broad spectrum of imaging appearances. Therefore, this review brings further support to a previously suggested denomination "Hantavirus disease" that would encompass all clinical manifestations (9,68). Although imaging won't show specific features in NE patients, knowledge of radiological appearances is useful to suggest or support a clinically suspected PUUV infection in the right clinical setting (fever, blurred vision, proteinuria, kidney failure

and thrombocytopenia, especially in endemic areas and patients at risk of exposure), before confirmation by serology.

References

1. Vapalahti O, Mustonen J, Lundkvist Å, et al. Hantavirus Infections in Europe. Lancet Infect Dis 2003;3:653–661.

2. Paakkala A, Mäkelä S, Hurme M, et al. Association of chest radiography findings with host-related genetic factors in patients with nephropathia epidemica. Scand J Infect Dis 2008;40:254–258.

3. Brummer-Korvenkontio M, Vaheri A, Hovi T, et al. Nephropathia Epidemica: Detection of Antigen in Bank Voles and Serologic Diagnosis of Human Infection. J Infect Dis 1980;141:131–134.

4. Mustonen J, Mäkelä S, Outinen T, et al. The pathogenesis of nephropathia epidemica: New knowledge and unanswered questions. Antiviral Res 2013;100:589–604.

5. Mustonen J, Brummer-Korvenkontio M, Hedman K, et al. Nephropathia Epidemica in Finland: A Retrospective Study of 126 Cases. Scand J Infect Dis 1994;26:7–13.

6. Hujakka H, Koistinen V, Kuronen I, et al. Diagnostic rapid tests for acute hantavirus infections: specific tests for Hantaan, Dobrava and Puumala viruses versus a hantavirus combination test. J Virol Methods 2003;108:117–122.

7. Kallio-Kokko H, Vapalahti O, Lundkvist Å, et al. Evaluation of Puumala virus IgG and IgM enzyme immunoassays based on recombinant baculovirus-expressed nucleocapsid protein for early nephropathia epidemica diagnosis. Clin Diagn Virol 1998;10:83–90.

8. Vaheri A, Henttonen H, Voutilainen L, et al. Hantavirus infections in Europe and their impact on public health: Hantavirus infections in Europe. Rev Med Virol 2013;23:35–49.

9. Clement J, Maes P, Lagrou K, et al. A unifying hypothesis and a single name for a complex globally emerging infection: hantavirus disease. Eur J Clin Microbiol Infect Dis 2012;31:1–5.

10. Clement J, Heyman P, McKenna P, et al. The hantaviruses of Europe: from the bedside to the bench. Emerg Infect Dis 1997;3:205–211.

11. Piechotowski I, Brockmann SO, Schwarz C, et al. Emergence of hantavirus in South Germany: rodents, climate and human infections. Parasitol Res 2008;103:131–137.

12. Tersago K, Verhagen R, Servais A, et al. Hantavirus disease (nephropathia epidemica) in Belgium: effects of tree seed production and climate. Epidemiol Infect 2009;137:250.

13. Kitterer D, Segerer S, Alscher MD, et al. Puumala Hantavirus-Induced Hemorrhagic Fever with Renal Syndrome Must Be Considered across the Borders of Nephrology to Avoid Unnecessary Diagnostic Procedures. PLOS ONE 2015;10:e0144622.

14. Partanen T, Koivikko M, Leisti P, et al. Long-term hormonal follow-up after human Puumala hantavirus infection. Clin Endocrinol (Oxf) 2016;84:85–91.

15. Jost C, Krause R, Graninger W, et al. Transient hypopituitarism in a patient with nephropathia epidemica. BMJ Case Rep;2009 . Epub ahead of print 2009.

16. Hautala T, Mähönen S-M, Sironen T, et al. Central nervous system-related symptoms and findings are common in acute Puumala hantavirus infection. Ann Med 2010;42:344–351.

17. Valtonen M, Kauppila M, Kotilainen P, et al. Four Fatal Cases of nephropathia epidemica. Scand J Infect Dis 1995;27:515–517.

18. Hautala T, Hautala N, Mähönen S-M, et al. Young male patients are at elevated risk of developing serious central nervous system complications during acute Puumala hantavirus infection. BMC Infect Dis;11 . Epub ahead of print December 2011.

19. Hautala T, Sironen T, Vapalahti O, et al. Hypophyseal Hemorrhage and Panhypopituitarism during Puumala Virus Infection: Magnetic Resonance Imaging and Detection of Viral Antigen in the Hypophysis. Clin Infect Dis 2002;35:96–101.

20. Tarvainen M, Mäkelä S, Mustonen J, et al. Autoimmune polyendocrinopathy and hypophysitis after Puumala hantavirus infection. Endocrinol Diabetes Metab Case Rep;2016 . Epub ahead of print November 4, 2016.

21. Settergren B, Boman J, Linderholm M, et al. A Case of Nephropathia Epidemica Associated with Panhypopituitarism and Nephrotic Syndrome. Nephron 1992;61:234–235.

22. Pekic S, Cvijovic G, Stojanovic M, et al. Hypopituitarism as a Late Complication of Hemorrhagic Fever. Endocrine 2005;26:079–082.

23. Forslund T, Saltevo J, Anttinen J, et al. Complications of nephropathia epidemica: three cases. J Intern Med 1992;232:87–90.

24. Mäkelä S, Jaatinen P, Miettinen M, et al. Hormonal deficiencies during and after Puumala hantavirus infection. Eur J Clin Microbiol Infect Dis 2010;29:705–713.

25. Steiner T, Ettinger J, Peng Z, et al. Hyperintense lesion in the corpus callosum associated with Puumala hantavirus infection. J Neurol 2012;259:1742–1745.

26. Bergmann F, Krone B, Bleich S, et al. Encephalitis due to a Hantavirus Infection. J Infect 2002;45:58–59.

27. [Anonymous 2019] Details omitted for double-blind reviewing.

28. Starkey J, Kobayashi N, Numaguchi Y, et al. Cytotoxic Lesions of the Corpus Callosum That Show Restricted Diffusion: Mechanisms, Causes, and Manifestations. RadioGraphics 2017;37:562–576.

29. Toivanen A-L, Valanne L, Tatlisumak T. Acute disseminated encephalomyelitis following nephropathia epidemica. Acta Neurol Scand 2002;105:333–336.

30. Krause R, Aberle S, Haberl R, et al. Puumala Virus Infection with Acute Disseminated Encephalomyelitis and Multiorgan Failure. Emerg Infect Dis 2003;9:603–605.

31. Kontkanen M, Puustjarvi T, Lahdevirta J. Myopic shift and its mechanism in nephropathia epidemica or Puumala virus infection. Br J Ophthalmol 1994;78:903–906.

32. Settergren B, Juto P, Trollfors B, et al. Clinical Characteristics of Nephropathia Epidemica in Sweden: Prospective Study of 74 Cases. Rev Infect Dis 1989;11:921–927.

33. Nguyên AT, Penalba C, Bernadac P, et al. [Respiratory manifestations of hemorrhagic fever with renal syndrome. Retrospective study of 129 cases in Champagne-Ardenne and Lorraine]. Presse Medicale Paris Fr 1983 2001;30:55–58.

34. Kanerva M, Paakkala A, Mustonen J, et al. Pulmonary involvement in nephropathia epidemica: radiological findings and their clinical correlations. Clin Nephrol 1996;46:369–378.

35. Mäkelä S, Kokkonen L, Ala-Houhala I, et al. More than half of the patients with acute Puumala hantavirus infection have abnormal cardiac findings. Scand J Infect Dis 2009;41:57–62.

36. Paakkala A, Lempinen L, Paakkala T, et al. Medical imaging in nephropathia epidemica and their clinical correlations. Eur J Intern Med 2004;15:284–290.

37. Paakkala A, Järvenpää R, Mäkelä S, et al. Pulmonary high-resolution computed tomography findings in nephropathia epidemica. Eur J Radiol 2012;81:1707–1711.

38. Linderholm M, Settergren B, Tärnvik A, et al. Pulmonary involvement in nephropathia epidemica as demonstrated by computed tomography. Infection 1992;20:263–266.

39. Rasmuson J, Lindqvist P, Sörensen K, et al. Cardiopulmonary involvement in Puumala hantavirus infection. BMC Infect Dis;13 . Epub ahead of print December 2013.

40. Paakkala A, Mustonen J. Radiological findings and their clinical correlations in nephropathia epidemica. Acta Radiol 2007;48:345–350.

41. Rasmuson J, Andersson C, Norrman E, et al. Time to revise the paradigm of hantavirus syndromes? Hantavirus pulmonary syndrome caused by European hantavirus. Eur J Clin Microbiol Infect Dis 2011;30:685–690.

42. Sargianou M, Watson DC, Chra P, et al. Hantavirus infections for the clinician: From case presentation to diagnosis and treatment. Crit Rev Microbiol 2012;38:317–329.

43. Duchin JS, Koster FT, Peters CJ, et al. Hantavirus pulmonary syndrome: a clinical description of 17 patients with a newly recognized disease. The Hantavirus Study Group. N Engl J Med 1994;330:949–955.

44. Signs & Symptoms | Hantavirus | DHCPP | CDC Available from: https://www.cdc.gov/hantavirus/hps/symptoms.html. 2019. Accessed March 25, 2019.

45. Clement J, Colson P, McKenna P. Hantavirus pulmonary syndrome in New England and Europe. N Engl J Med 1994;331:545–546; author reply 547-548.

46. Gizzi M, Delaere B, Weynand B, et al. Another case of "European hantavirus pulmonary syndrome" with severe lung, prior to kidney, involvement, and diagnosed by viral inclusions in lung macrophages. Eur J Clin Microbiol Infect Dis 2013;32:1341–1345.

47. Fakhrai N, Mueller-Mang C, El-Rabadi K, et al. Puumala Virus Infection: Radiologic Findings. J Thorac Imaging 2011;26:W51–W53.

48. Caramello P, Canta F, Bonino L, et al. Puumala Virus Pulmonary Syndrome in a Romanian Immigrant. J Travel Med 2006;9:326–329.

49. Krumm P, Zitzelsberger T, Gawaz M, et al. Young patient with hantavirus-induced myocarditis detected by comprehensive cardiac magnetic resonance assessment. BMC Infect Dis;19 . Epub ahead of print December 2019.

50. Mustonen J, Helin H, Pietilä K, et al. Renal biopsy findings and clinicopathologic correlations in nephropathia epidemica. Clin Nephrol 1994;41:121–126.

51. Remer EM, Papanicolaou N, Casalino DD, et al. ACR Appropriateness Criteria® on Renal Failure. Am J Med 2014;127:1041-1048.e1.

52. Paakkala A, Kallio T, Huhtala H, et al. Renal ultrasound findings and their clinical associations in Nephropathia epidemica. Analysis of quantitative parameters. Acta Radiol 2002;43:320–325.

53. Paakkala A, Kallio T, Huhtala H, et al. Value of ultrasonography in acute renal failure: analysis of qualitative features in patients with nephropathia epidemica. Acta Radiol 2004;45:785–790.

54. Glodny B, Unterholzner V, Taferner B, et al. Normal kidney size and its influencing factors - a 64-slice MDCT study of 1.040 asymptomatic patients. BMC Urol;9 . Epub ahead of print December 2009.

55. Emamian SA, Nielsen MB, Pedersen JF, et al. Kidney dimensions at sonography: correlation with age, sex, and habitus in 665 adult volunteers. Am J Roentgenol 1993;160:83–86.

56. Paakkala A, Dastidar P, Ryymin P, et al. Renal MRI findings and their clinical associations in nephropathia epidemica: analysis of quantitative findings. Eur Radiol 2005;15:968–974.

57. Scheirey CD, Fowler KJ, Therrien JA, et al. ACR Appropriateness Criteria® Acute Nonlocalized Abdominal Pain. J Am Coll Radiol 2018;15:S217–S231.

58. Kim YO, Chun KA, Choi JY, et al. Sonographic evaluation of gallbladder-wall thickening in hemorrhagic fever with renal syndrome: Prediction of disease severity. J Clin Ultrasound 2001;29:286–289.

59. Nicolas JB. Acalculous cholecystitis associated with hemorrhagic fever with renal syndrome. Acta Clin Belg 2015;70:377–381.

60. Keyaerts E, Ghijsels E, Lemey P, et al. Plasma Exchange--Associated Immunoglobulin M--Negative Hantavirus Disease after a Camping Holiday in Southern France. Clin Infect Dis 2004;38:1350–1356.

61. Koskela SM, Laine OK, Paakkala AS, et al. Spleen enlargement is a common finding in acute Puumala hantavirus infection and it does not associate with thrombocytopenia. Scand J Infect Dis 2014;46:723–726.

62. Chow KU, Luxembourg B, Seifried E, et al. Spleen Size Is Significantly Influenced by Body Height and Sex: Establishment of Normal Values for Spleen Size at US with a Cohort of 1200 Healthy Individuals. Radiology 2016;279:306–313.

63. Spielmann AL, DeLong DM, Kliewer MA. Sonographic Evaluation of Spleen Size in Tall Healthy Athletes. Am J Roentgenol 2005;184:45–49.

64. Kitterer D, Artunc F, Segerer S, et al. Evaluation of lipase levels in patients with nephropathia epidemica - no evidence for acute pancreatitis. BMC Infect Dis;15 . Epub ahead of print December 2015.

65. Huttunen N-P, Mäkelä S, Pokka T, et al. Systematic literature review of symptoms, signs and severity of serologically confirmed nephropathia epidemica in paediatric and adult patients. Scand J Infect Dis 2011;43:405–410.

66. Puca E, Pilaca A, Pipero P, et al. Hemorrhagic fever with renal syndrome associated with acute pancreatitis. Virol Sin 2012;27:214–217.

67. Zhu Y, Chen Y-X, Zhu Y, et al. A retrospective study of acute pancreatitis in patients with hemorrhagic fever with renal syndrome. BMC Gastroenterol;13 . Epub ahead of print December 2013.

68. Desmyter J, Van Ypersele De Strihou C, Van Der Groen G. HANTAVIRUS DISEASE. The Lancet 1984;324:158.

Figures

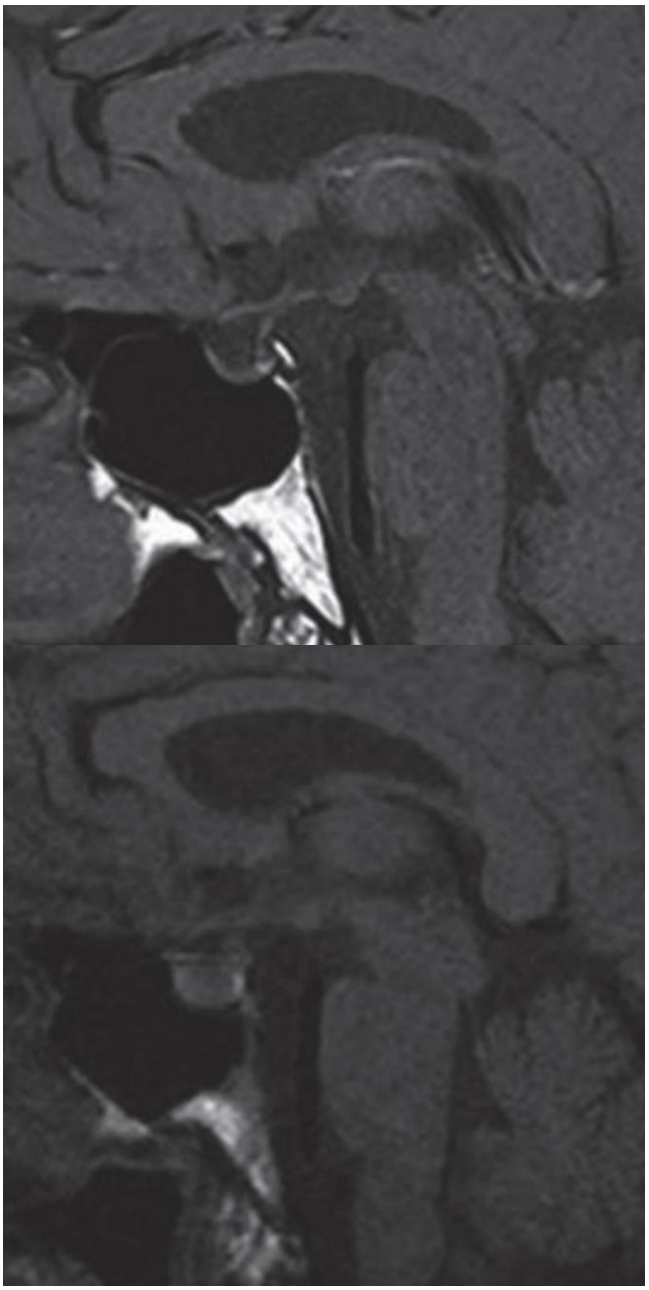

Figure 1. T1-weighted sagittal MRI during the acute phase (a) displays an increased signal intensity in the pituitary gland consistent with hemorrhage. Control MRI (b) shows an atrophic pituitary gland. The sagittal diameter of the pituitary gland had been markedly reduced from 9.1 mm (a) to 1.9 mm (b). Republished with permission of John Wiley and Sons, from (14); permission conveyed through Copyright Clearance Center, Inc.

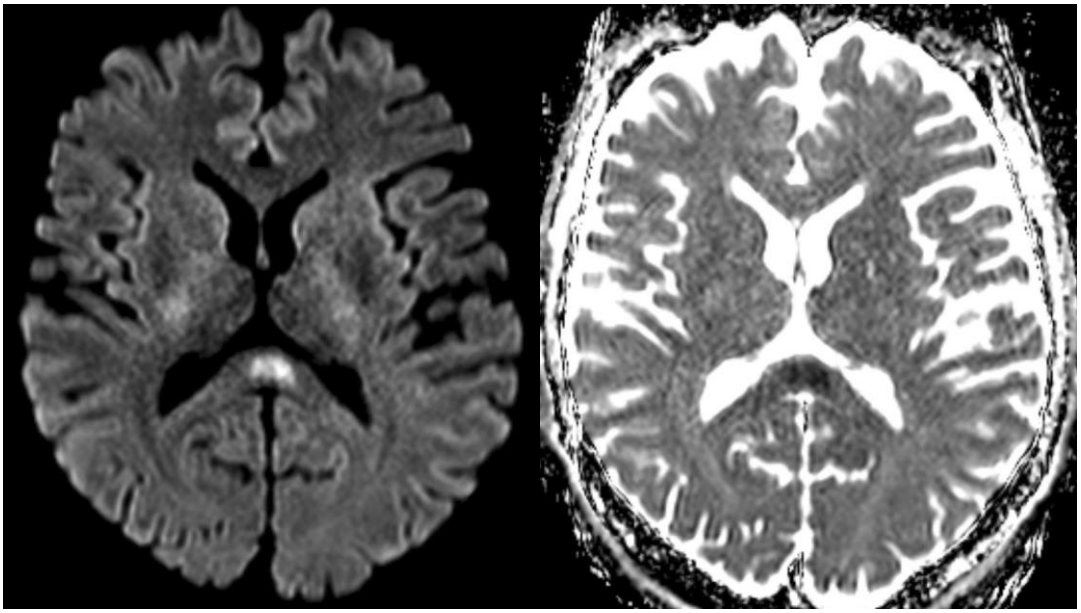

Figure 2. Brain MRI axial diffusion-weighted image (b = 1000 s/mm2) (left) shows a high signal intensity in the splenium of corpus callosum. Apparent diffusion coefficient (ADC) map image (right) shows a low ADC. This image was originally published with a CC BY licence (27).

Figure 3. Chest X-ray, posteroanterior view, shows slight right-sided pleural effusion and cardiac enlargement.

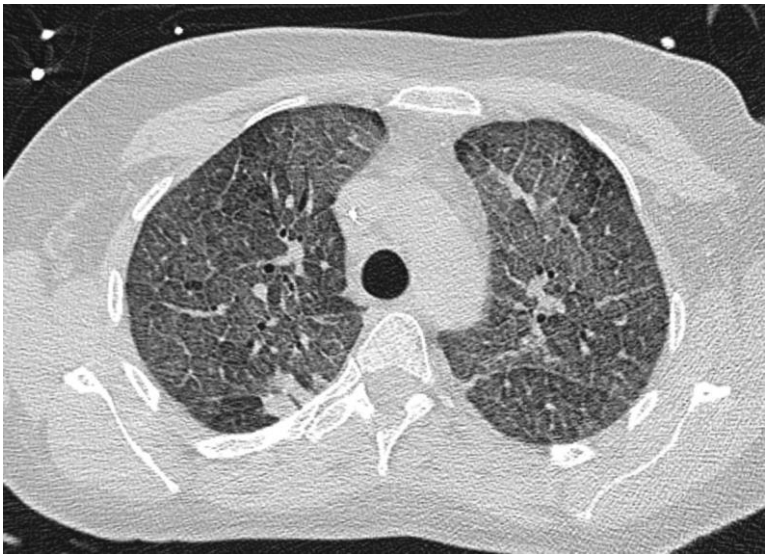

Figure 4. Chest high-resolution CT, lung window, shows diffuse interlobular septal thickening, GGOs (crazy-paving pattern), and a right upper lobe condensation.

Figure 5. Kidney US shows increased cortical echogenicity, increased cortical parenchymal thickness, and decreased corticomedullary border differentiation.

Figure 6. Kidney US shows perirenal fluid.

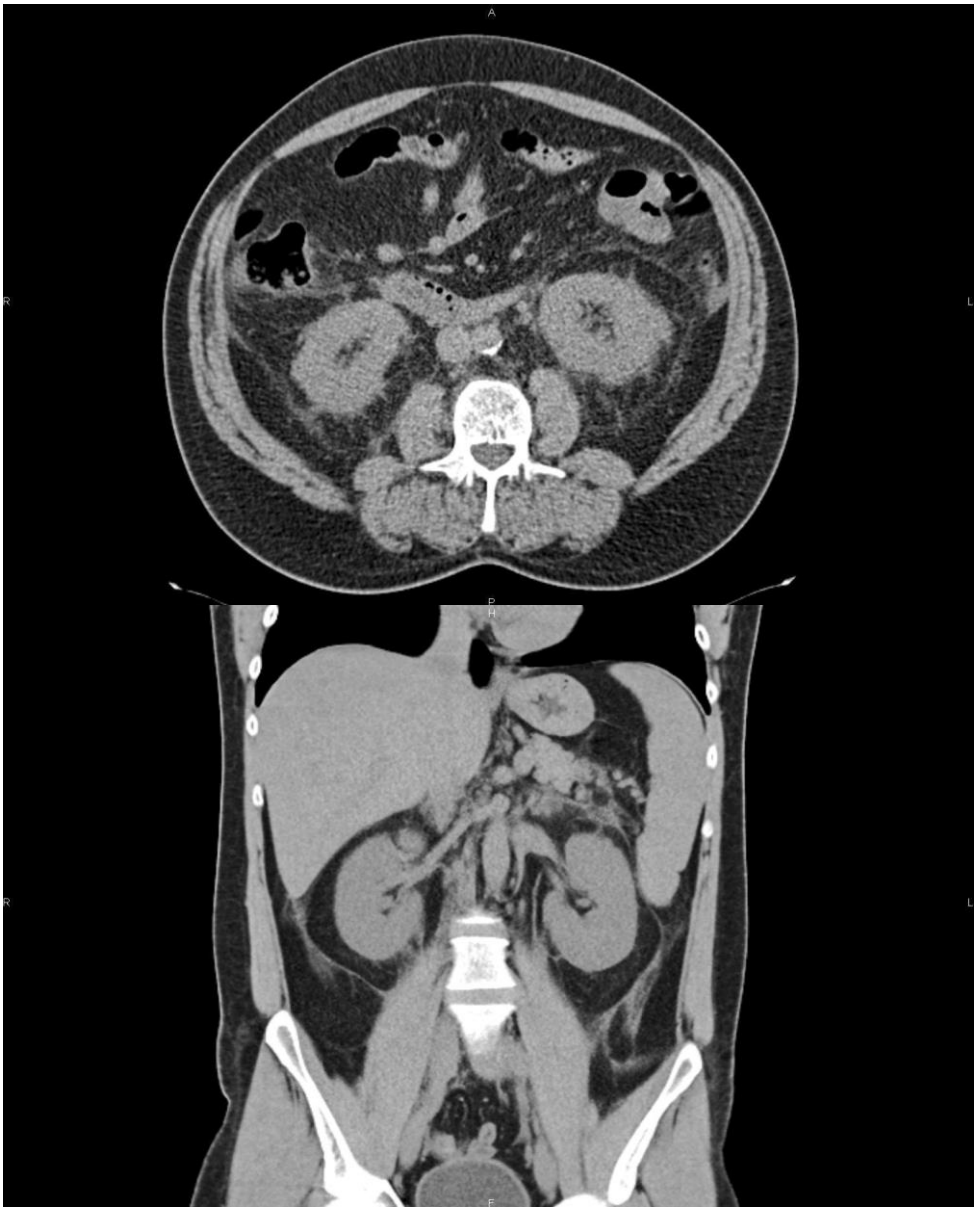

Figure 7. Unenhanced abdominal CT, axial (a) and coronal (b) sections (different patients). Axial image (a) shows stranding of the perinephric fat as well as outside the perirenal fascia. Coronal image (b) shows similar findings, with splenomegaly (15.7 cm).

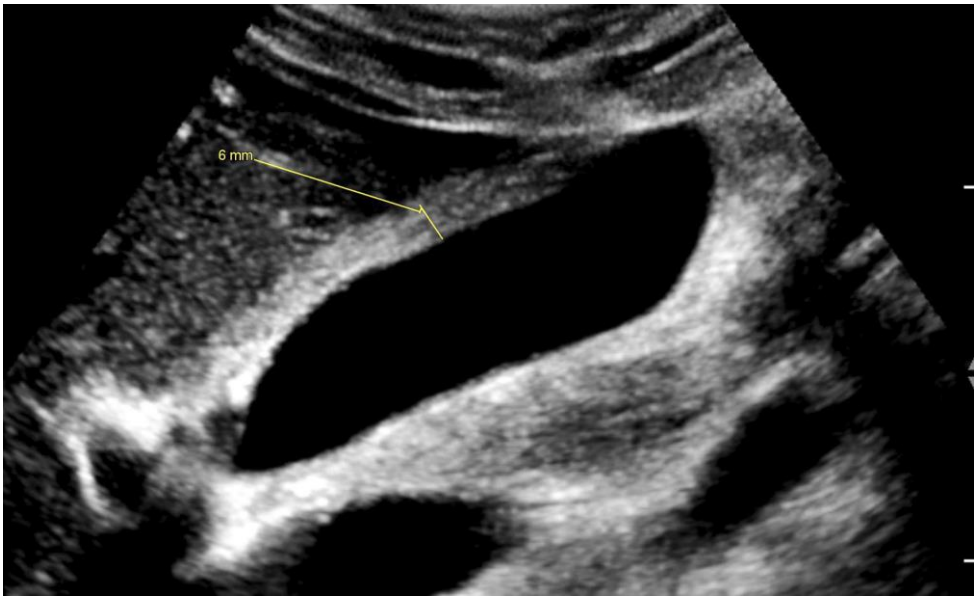

Figure 8. Longitudinal US of the gallbladder shows gallbladder-wall thickening (6 mm).